Direct characterization of quantum dynamics with single-photon two-qubit states

Wei-Tao Liu,* Wei Wu, Ping-Xing Chen, Cheng-Zu Li, and Jian-Min Yuan
Department of Physics, National University of Defense Technology, Changsha, 410073, People's Republic of China
(Received 6 December 2007; published 19 March 2008)

Direct characterization of quantum dynamics (DCQD) introduced by Mohseni and Lidar [Phys. Rev. Lett. **97**, 170501 (2006)] offers an effective way for estimation of quantum dynamical systems. Employing single-photon two-qubit states, we experimentally implement DCQD of one-qubit dynamics. The requirement of two-body interactions is thus eliminated such that the algorithm can be realized more conveniently. Both DCQD and standard quantum process tomography (SQPT) measurements are performed for several processes. The data from both methods show good agreement. Although the average process fidelities of the data obtained via DCQD are a little lower than that of SQPT, the number of experimental configurations is quadratically reduced evidencing the quadratic advantage of DCQD scheme. Partial information of the quantum dynamics can also be directly extracted via DCQD with fewer measurements.

DOI: 10.1103/PhysRevA.77.032328 PACS number(s): 03.67.Mn, 42.50.Dv, 42.65.Lm

I. INTRODUCTION

Quantum-information science [1] offers a way for more efficient and secure information processing, by properly controlling and measuring on certain quantum systems. Unfortunately, the states of the quantum systems are often fragile, especially when the systems are involved in unknown interactions with the environment. Accurate estimation and control on the quantum systems in the presence of decoherence are thus important, for which the knowledge of the quantum dynamics acting on the quantum system is indispensable. Therefore the characterization of quantum dynamical systems becomes a task of fundamental and practical importance, which provides the required knowledge for estimation and control on the quantum dynamics, especially for verifying or monitoring the performance of a quantum device, and the design of decoherence-mitigation methods. One usual method for this characterization is standard quantum process tomography (SQPT) [1–6]. An ensemble of identical quantum systems are prepared in a member of a set of quantum states, then each of them are subjected to the concerned quantum dynamics, and the dynamical process is reconstructed by quantum state tomography [7] on the output. Another method is known as ancilla-assisted process tomography (AAPT) [8–12], extracting the information of dynamics by performing quantum state tomography on the joint system of the primary system and ancilla.

However, the total number of experimental configurations for measurements grows exponentially with the degrees of freedom of the system, and the information is acquired indirectly. To address these issues, Mohseni and Lidar [13] proposed an algorithm for direct characterization of quantum dynamics (DCQD). The primary system is initially entangled with an ancilla system, and subjected to the concerned quantum dynamics, then information about the dynamics is acquired through a certain set of error-detecting measurements. The number of experimental configurations is reduced quadratically compared to that of SQPT and separable AAPT [13,14]. Considering characterization of one-qubit quantum dynamics, by inputting four two-qubit entangled states into the quantum dynamics and performing certain Bell-state measurements (BSMs) on the outputs, the information about the dynamics can be completely obtained. The number of required experimental configurations is four for DCQD, while 16 for both SQPT and separable AAPT. For quantum dynamics of multiqubit systems, the quadratic advantage is more obvious. Furthermore, information of quantum dynamics is acquired directly, therefore DCQD can be used to extract partial information of the quantum dynamics with fewer measurements [13,14], when we do not need the full characterization of quantum dynamics or we have *a priori* knowledge about the concerned system. In practice, DCQD has important application in characterization of quantum systems embedded with unknown interactions with the environment. It is more convenient and practical since the information of quantum dynamics can be acquired directly with fewer measurements.

Direct characterization of one-qubit quantum dynamics has been experimentally demonstrated with two-photon polarization entangled states [15]. Due to the lack of complete Bell-state discrimination system, the number of experimental configurations is only reduced by a factor of 2. Besides, in both theoretical discussions [13,14] and the experiment [15], two-body interactions are required for DCQD of one-qubit dynamics.

In the present work, we implement the task with a practical scheme, which makes DCQD of one-qubit dynamics more convenient. Employing single-photon two-qubit states [16], two-body interactions are no longer required. In the experiment, one-qubit dynamics acting on the polarization state of a photon is considered. With polarization qubit of the photon being the primary system while spatial (path) qubit being the ancilla, deterministic Bell-state measurements become easy to be carried out and the number of experimental configurations is reduced to four, revealing the quadratic advantage of the algorithm. Moreover, since all the operations and measurements are performed on single-photon states, the DCQD algorithm for one-qubit dynamics becomes more convenient to be realized. In the experiment, we perform DCQD measurements for several quantum dynamics simu-

*mugualaw@hotmail.com

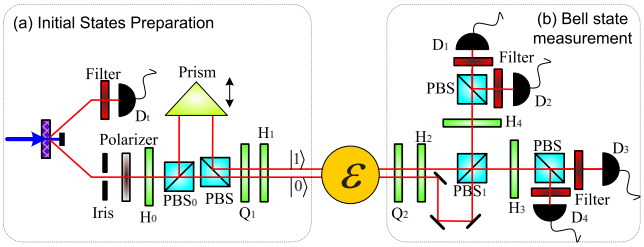

FIG. 1. (Color online) The experimental setup for direct characterization of quantum dynamics with single-photon two-qubit states. $H(Q)$: Half- (quarter-) wave plate; D, avalanche photodiodes (APD). (a) Preparation of input states. Heralded single photons created via spontaneous parametric down conversion are prepared in the state $|H\rangle$ by the polarizer. Then the required entangled states are prepared by properly setting the wave plates (shown in Table I). (b) Bell-state measurements on the output, performed via a polarization beam splitter (PBS_1) and the following polarization analysis. The preparation and BSM stages form a balanced Mach-Zehnder interferometer.

lated with some optical devices. The average process fidelities of the experimental data for all of the concerned processes are higher than 97.4%. For the same processes, SQPT measurements are also performed for comparison and the data obtained via two methods are in good agreement.

II. DCQD WITH SINGLE-PHOTON TWO-QUBIT STATES

The evolution of a one-qubit quantum system can be expressed in terms of a completely positive quantum dynamical map ε, which can be represented as [1]

$$\varepsilon(\rho) = \sum_{m,n=0}^{3} \chi_{mn} E_m \rho E_n^{\dagger}, \tag{1}$$

where ρ is the initial state of the system, and $\{E_m\}$ are selected as the error operator basis identity operator and Pauli operators, $\{I,X,Y,Z\}$. $\{\chi_{mn}\}$ are the matrix elements of the superoperator χ, which contains all of the information about the quantum dynamics. The task is to determine each element of the matrix χ directly in the experiment.

To determine the diagonal elements of χ, the initial state is prepared in the maximally entangled state

$$|\phi^+\rangle = (|H\rangle|0\rangle + |V\rangle|1\rangle)/\sqrt{2} \tag{2}$$

where $|H\rangle$ ($|V\rangle$) represents the horizontal (vertical) polarization state, while $\{|0\rangle,|1\rangle\}$ refer to the spatial qubit of the photon (see Fig. 1). Then we subject the polarization qubit to the map ε, and perform measurements of the observables ZZ and XX, which is equivalent to BSM. The probabilities of obtaining different output states become

$$p_{mZ} = \mathrm{Tr}[P_{mZ}\varepsilon(\rho)] = \chi_{mm} \quad (m = 0,1,2,3), \tag{3}$$

where

$$P_{0Z} = |\phi^+\rangle\langle\phi^+|, \quad P_{1Z} = |\psi^+\rangle\langle\psi^+|,$$

$$P_{2Z} = |\psi^-\rangle\langle\psi^-|, \quad P_{3Z} = |\phi^-\rangle\langle\phi^-| \tag{4}$$

are the four Bell-state projection operators with $|\phi^{\pm}\rangle = (|H\rangle|0\rangle \pm |V\rangle|1\rangle)/\sqrt{2}$ and $|\psi^{\pm}\rangle = (|H\rangle|1\rangle \pm |V\rangle|0\rangle)/\sqrt{2}$.

In order to obtain the off-diagonal elements of χ, a set of BSMs should be performed to acquire only partial information about the system. For instance, to determine χ_{03} and χ_{12}, the initial input state is modified into

$$|\psi_Z\rangle = \alpha|H0\rangle + \beta|V1\rangle \tag{5}$$

with $|\alpha| \neq |\beta| \neq 0$. With the results of Bell-state projection measurements performed on the output, we obtain

$$\begin{aligned}
&\mathrm{Re}(\chi_{03})U = \mathrm{Tr}[P_{0Z}\varepsilon(\rho)] + \mathrm{Tr}[P_{3Z}\varepsilon(\rho)] - \chi_{00} - \chi_{33},\\
&\mathrm{Im}(\chi_{03})N = \mathrm{Tr}[P_{0Z}\varepsilon(\rho)] - \mathrm{Tr}[P_{3Z}\varepsilon(\rho)] - M(\chi_{00} - \chi_{33}),\\
&\mathrm{Im}(\chi_{12})U = \mathrm{Tr}[P_{1Z}\varepsilon(\rho)] + \mathrm{Tr}[P_{2Z}\varepsilon(\rho)] - \chi_{11} - \chi_{22},\\
&\mathrm{Re}(\chi_{12})N = \mathrm{Tr}[P_{2Z}\varepsilon(\rho)] - \mathrm{Tr}[P_{1Z}\varepsilon(\rho)] + M(\chi_{11} - \chi_{22}),
\end{aligned} \tag{6}$$

with $U=2(|\alpha|^2-|\beta|^2)$, $M=2\,\mathrm{Re}(\alpha\beta^*)$, and $N=4\,\mathrm{Im}(\alpha\beta^*)$.

To characterize the remaining off-diagonal elements of χ, the basis of the input states and measurements must be transformed. To determine χ_{01} and χ_{23}, the input state is changed into

$$|\psi_X\rangle = \alpha|+\rangle|0\rangle + \beta|-\rangle|1\rangle \tag{7}$$

with $|\pm\rangle = (|H\rangle \pm |V\rangle)/\sqrt{2}$. BSM is accordingly transformed as the measurements of observables XZ and ZX. The results have similar form to Eq. (6).

To determine χ_{02} and χ_{13}, the input is prepared as

$$|\psi_Y\rangle = \alpha|+i\rangle|0\rangle + \beta|-i\rangle|1\rangle \tag{8}$$

with $|\pm i\rangle = (|H\rangle \pm i|V\rangle)/\sqrt{2}$ and the BSM operators are YZ and ZY. Then the matrix χ, thus the full information about the concerned quantum dynamics, can be directly obtained with four different inputs and corresponding BSMs.

III. EXPERIMENT

The experimental setup is shown in Fig. 1. Spontaneous parametric down-conversion (SPDC) process is employed to prepare heralded single photons [17,18]. A mode-locked Ti-:sapphire pulsed laser (with the pulse width less than 200 fs, the repetition about 76 MHz, and the center wavelength at 850 nm) is frequency doubled to produce the pumping source. The average power of the pump source is 600 mW. A 1.0-mm-thick β-barium borate nonlinear crystal cut for type-II noncollinear phase match is used as the down converter. The photons are detected at a wavelength of 850 nm through interference filters with a $\Delta\lambda_{\mathrm{FWHM}}=10$ nm, which results in a coherence time of 240 fs. As the photons of a pair are strongly correlated in time, the detection of one photon heralds the existence of the other one which is used for the scheme. Coincidence detection is performed between D_t and D_i $(i=1,2,3,4)$, within a chosen time window of 2 ns. In

TABLE I. The settings of the wave plates in our experiment. The numerals show angles of the fast axes of the wave plates, with respect to the vertical axis. All of the wave plates are not simultaneously used in a single experiment configuration.

Required input	H_0	Q_1	H_1	Q_2	H_2
$\|\phi^+\rangle$	67.5°°				
$\|\psi_Z\rangle$	75°	90°			
$\|\psi_X\rangle$	75°	90°	−22.5°		−22.5°
$\|\psi_Y\rangle$	75°	45°		−45°	

addition, the probability of producing more than one pair during a single pump pulse is much less than that of only one pair. Accidental coincidences or multicoincidences are thus negligible. The single photons are then prepared into the state $|H\rangle$ via a polarizer [shown in Fig. 1(a)].

For obtaining the diagonal elements of χ, the initial state $|\phi^+\rangle$ is prepared by lighting single photons polarized in the state $|+\rangle$ onto a polarization beam splitter (PBS, transmitting horizontal polarized light and reflecting vertical ones) [16], setting the fast axis of the half-wave plate H_0 at an angle of 67.5° with respect to the vertical axis. Then we subject the polarization qubit of the photons to the quantum dynamics ε and perform BSM on the outputs. For deterministic Bell-state discrimination, PBS_1 and polarization measurements in the basis $\{|\pm\rangle\}$ (with the half-wave plates H_3 and H_4 set at 67.5°) are employed, shown in Fig. 1(b). The two paths are recombined on PBS_1, which performs as a controlled-NOT (CNOT) gate with the polarization state of the photon being the control qubit and the spatial qubit being the target [19,20]. The preparation and measurement stages form an equal-path Mach-Zehnder interferometer. A prism is employed to compensate the optical path difference and ensure the interference of the two paths on PBS_1. For characterizing the off-diagonal elements of χ, we choose $\alpha=\sqrt{3}/2$ and $\beta=i/2$. Another two half-wave plates ($H_{1,2}$) or quarter-wave plates ($Q_{1,2}$) are employed. By properly setting these wave plates (shown in Table I), the required input states and the BSMs are successfully achieved.

IV. RESULTS AND DISCUSSIONS

In the experiment, we investigate several quantum dynamical processes, including three trace-preserving maps (identity and two unitary rotation operators) and one non-trace-preserving map (a polarizer). A half-wave plate is selected and inserted into the place of ε to simulate two unitary operators. By setting its fast axis at an angle of −45° with respect to the vertical axis, X gate is simulated first. Then the angle of the half-wave plate is set at −22.5° to simulate a Hadamard gate [1]. For the non-trace-preserving map, a polarizer set to transmit only horizontal polarized light is concerned. In the experiment, the Bell-state preparations and measurements are sensitive to the relative phase in two arms of Mach-Zehnder interferometer. So the interferometer should be aligned to be absolutely balanced without any phase fluctuation in two arms, which is impossible in practical. We try to meet this request by keeping the visibility of the interferometer as stable as possible. The interferometer is located in a box fixed on an air cushion table to reduce the phase fluctuation. During our experiment, the visibility varies slowly with time due to phase fluctuations and maintains above 97.8% within more than 10 minutes, which is long enough for us to complete the measurements. The experimental results of the DCQD measurements are converted into a positive and Hermitian matrix using the maximum-likelihood technique [21]. The real and imaginary part of the obtained matrix χ are shown in Fig. 2. To test whether the experimentally obtained matrix χ agrees with the concerned quantum dynamics, we calculate the average process fidelity [10] between the experimental data and the theoretical matrix. For identity map, the average process fidelity is

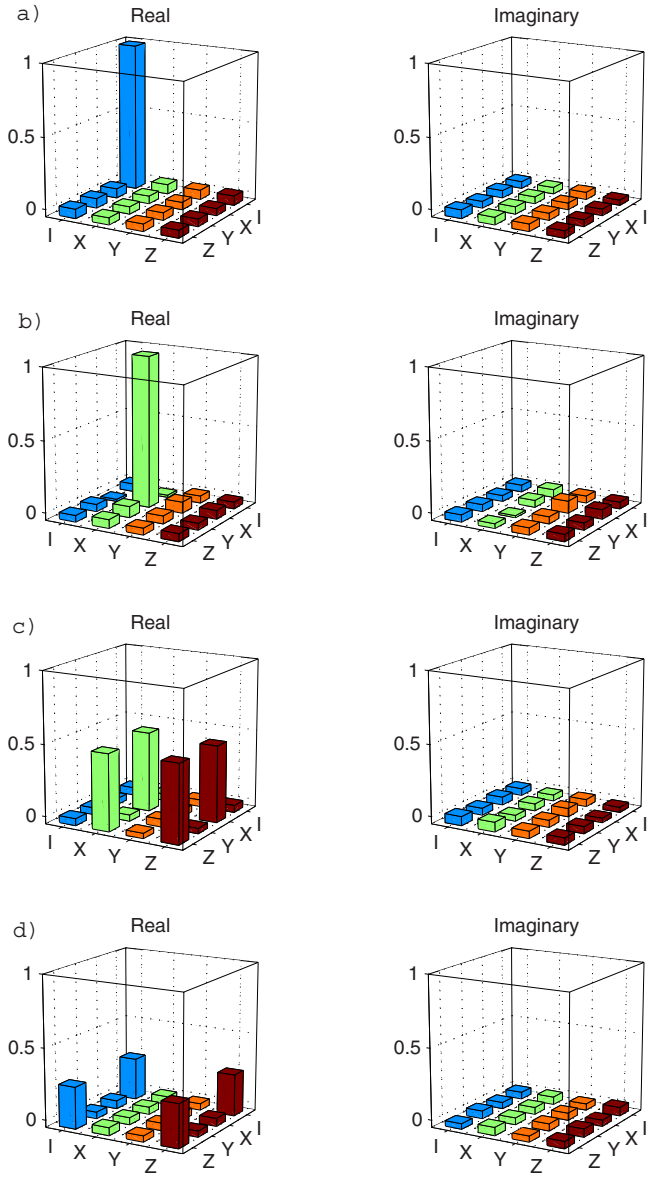

FIG. 2. (Color online) The matrix χ obtained from direct characterization of quantum dynamics (DCQD) for (a) identity, (b) unitary, X gate simulated with half-wave plate, (c) unitary, Hadamard gate simulated, (d) polarizer set to transmit only horizontal polarized light.

TABLE II. Average process fidelities for each process between the matrix obtained via DCQD, SQPT, and the theoretical matrix. F_{DT} in the table refers to the process fidelity between the matrix obtained via DCQD and the theoretical matrix, similarly for F_{DS}, F_{ST}.

	F_{DT}	F_{DS}	F_{ST}
Identity	$98.8\% \pm 0.6\%$	$98.9\% \pm 0.8\%$	$99.8\% \pm 0.4\%$
X gate	$97.4\% \pm 0.7\%$	$98.0\% \pm 0.6\%$	$99.4\% \pm 0.5\%$
Hadamard gate	$98.5\% \pm 0.5\%$	$97.6\% \pm 0.5\%$	$99.5\% \pm 0.3\%$
Polarizer	$97.8\% \pm 0.5\%$	$97.9\% \pm 0.5\%$	$99.8\% \pm 0.4\%$

$98.8\% \pm 0.6\%$ and the fidelities for other concerned processes are all higher than 97.4%, summarized as F_{DT} in Table II.

For the same processes, SQPT measurements are also performed for comparison. We prepare polarization qubits in the states of $\{|H\rangle, |V\rangle, |+\rangle, |+i\rangle\}$, then subject each of them to the map ε, perform quantum state tomography on the outputs and obtain the matrix χ using the method introduced in Ref. [1] and the maximum-likelihood technique [21]. The results are shown in Fig. 3 and the average process fidelities F_{ST} of the experimental data are shown in Table II.

By comparing the data shown in Figs. 2 and 3, we find the results of DCQD and that of SQPT agree well. The average process fidelities between these two methods (F_{DS}) for identity map is $98.9\% \pm 0.8\%$. For the unitary maps, the process fidelities are $98.0\% \pm 0.6\%$ and $97.6\% \pm 0.5\%$ for X gate and Hadamard gate, respectively. The fidelity for the polarizer is $97.9\% \pm 0.5\%$.

Although the average process fidelities of the data obtained via DCQD are a little lower than that of SQPT, the number of experimental configurations is quadratically reduced and partial information of the quantum dynamics can be directly extracted with fewer measurements. In the experiment, four different input states and corresponding Bell-state discriminations are required. Since BSMs can be deterministically performed here, only four experimental configurations are necessary thus the quadratic advantage of DCQD is revealed. We can also directly obtain certain elements of χ, such as χ_{mm}, with certain input and corresponding BSM without performing all four measurements. At the same time, the primary qubit and the ancilla are prepared on a single photon thus all the operations and measurements are performed on single-photon states. In addition, SPDC is not necessary for our scheme although it is used to create heralded single photons in the experiment. Other kinds of (quasi-) single-photon sources, such as faint laser pulses [22], colored centers in diamond [23,24], can also be used for this scheme. These issues make DCQD algorithm for one-qubit quantum dynamics more convenient to be performed in practice.

The major imperfection in the experiment may come from the following sources. The first one is the imperfection of the interferometer, which is mainly caused by phase fluctuation in two arms of Mach-Zehnder interferometer and imperfect overlap in the spatial modes. The second one is some practical imperfections in optical elements, especially the elements employed in the interferometer since the two beams light on them at different points.

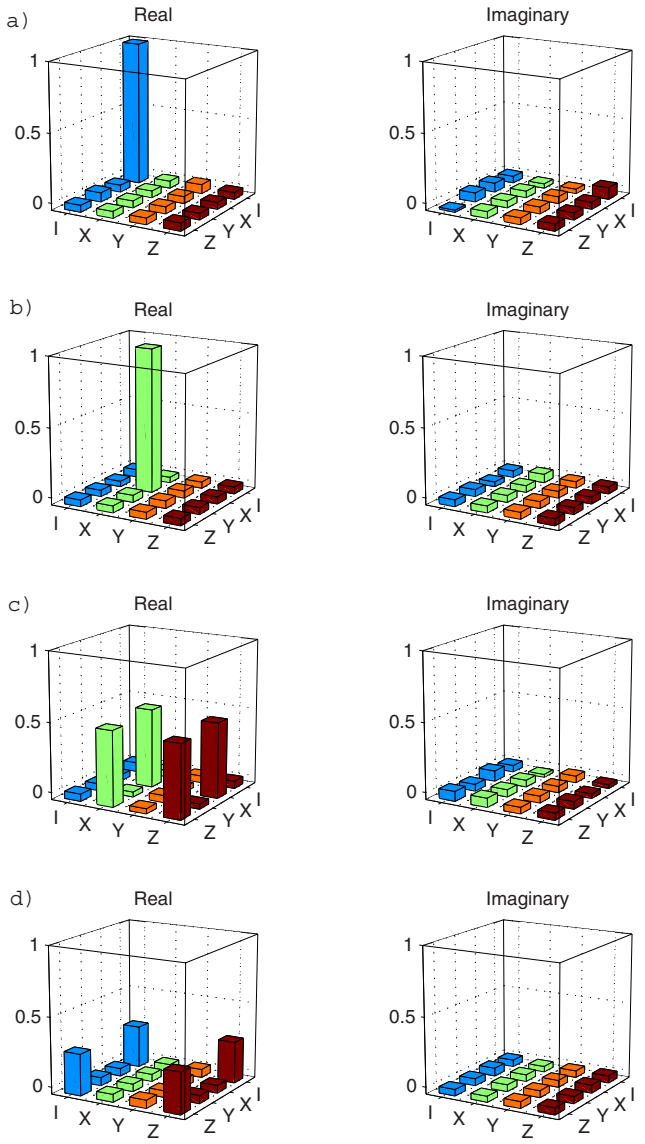

FIG. 3. (Color online) The matrix χ obtained from stand quantum process tomography (SQPT) for (a) identity, (b) unitary, X gate simulated with half-wave plate, (c) unitary, Hadamard gate simulated, (d) polarizer set to transmit only horizontal polarized light.

The quantum dynamics concerned in our experiment act only on the polarization state of the photon. Using single-photon two-qubit states and similar experimental arrangements, direct characterization of those dynamics acting on the spatial qubit can also be performed.

To subject the polarization qubit to the dynamics, the two beams (corresponding to paths $|0\rangle$ and $|1\rangle$ in Fig. 1) should transmit through the same devices whose dynamics are concerned. The two beams are parallel aligned with a distance of about 7 mm to light on the devices inserted into the place of ε, with the clear apertures of no less than 12.7 mm. In reality, there are some devices (for example, optical fibers) whose clear apertures are not large enough for two beams. For these devices, the above scheme can also work under slight modifications, as shown in Fig. 4. An optical switch (OS, as has

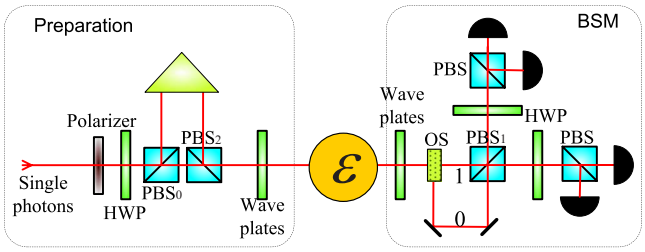

FIG. 4. (Color online) A modified scheme for devices whose clear apertures are not large enough. Temporally separated two parts of a single photon are recombined on the polarization beam splitter PBS_1 with the help of the optical switch (OS) after subjected to the quantum dynamics ε. Preparations and measurements of the states are similar to that of the original scheme.

been used in Ref. [25], for example) is introduced. Single-photon lighting on PBS_0 is divided into two parts, then combined into one single beam by PBS_2, with the two parts temporally separated due to a length difference of the two paths between PBS_0 and PBS_2. After subjecting to the map ε, the earlier part is lead into the longer path "0" via the optical switch, while the later part into the shorter path "1." Then two parts encounter on PBS_1 for interference and DCQD measurements can be achieved.

DCQD provides us an effective way for estimation of quantum dynamical systems. Some important physical quantities associated with the elements of χ can be directly determined and partial information about the dynamics can be extracted with fewer measurements. In practice, DCQD has important application in characterization of quantum systems, especially when the quantum systems are involved in unknown interactions with the environment. It can be used to accurately estimate those quantum devices and quantum channels employed in quantum computation and quantum communication, in order to verify or monitor the performance of them under decoherence. DCQD offers indispensable knowledge of the systems for prediction of outcomes and closed-loop control on the systems, which is important for quantum error correction [1] and coherent control [26]. It can also be applied to other fields in quantum-information science, such as Hamiltonian identification and generalized quantum dense coding tasks [14].

In summary, we experimentally implement DCQD algorithm for one-qubit quantum dynamics using single-photon two-qubit states. The experimental data offer high average process fidelities. For comparison, we also perform SQPT measurements, the results obtained via the two methods are in good agreement. In virtue of deterministic Bell-state discrimination on this kind of state, the quadratical advantage of DCQD is revealed with the number of experimental configurations reduced to four in our experiment. Direct characterization of one-qubit quantum dynamics is made more practical, since two-photon states manipulations and two-body interactions are no longer necessary in our scheme.

ACKNOWLEDGMENTS

The work was supported by National Natural Science Foundation of China (Grant Nos. 10774192 and 10504042) and Innovation Funds for Ph.D. candidates in the University.

[1] M. A. Nielsen and I. L. Chuang, *Quantum Computation and Quantum Information* (Cambridge University Press, Cambridge, UK, 2001).
[2] J. F. Poyatos, J. I. Cirac, and P. Zoller, Phys. Rev. Lett. **78**, 390 (1997).
[3] I. L. Chuang and M. A. Nielsen, J. Mod. Opt. **44**, 2455 (1997).
[4] A. M. Childs, I. L. Chuang, and D. W. Leung, Phys. Rev. A **64**, 012314 (2001).
[5] M. W. Mitchell, C. W. Ellenor, S. Schneider, and A. M. Steinberg, Phys. Rev. Lett. **91**, 120402 (2003).
[6] J. L. O'Brien, G. J. Pryde, A. Gilchrist, D. F. V. James, N. K. Langford, T. C. Ralph, and A. G. White, Phys. Rev. Lett. **93**, 080502 (2004).
[7] A. G. White, D. F. V. James, P. H. Eberhard, and P. G. Kwiat, Phys. Rev. Lett. **83**, 3103 (1999).
[8] G. M. D'Ariano and P. Lo Presti, Phys. Rev. Lett. **86**, 4195 (2001).
[9] D. W. Leung, J. Math. Phys. **44**, 528 (2003).
[10] J. B. Altepeter, D. Branning, E. Jeffrey, T. C. Wei, P. G. Kwiat, R. T. Thew, J. L. O'Brien, M. A. Nielsen, and A. G. White, Phys. Rev. Lett. **90**, 193601 (2003).
[11] G. M. D'Ariano and P. Lo Presti, Phys. Rev. Lett. **91**, 047902 (2003).
[12] F. DeMartini, A. Mazzei, M. Ricci, and G. M. D'Ariano, Phys. Rev. A **67**, 062307 (2003).
[13] M. Mohseni and D. A. Lidar, Phys. Rev. Lett. **97**, 170501 (2006).
[14] M. Mohseni and D. A. Lidar, Phys. Rev. A **75**, 062331 (2007).
[15] Z. W. Wang, Y. S. Zhang, Y. F. Huang, X. F. Ren, and G. C. Guo, Phys. Rev. A **75**, 044304 (2007).
[16] Y. H. Kim, Phys. Rev. A **67**, 040301(R) (2003).
[17] C. K. Hong and L. Mandel, Phys. Rev. Lett. **56**, 58 (1986).
[18] T. Pittman, B. Jacobs, and J. Franson, Opt. Commun. **246**, 545 (2005).
[19] Y. F. Huang, X. F. Ren, Y. S. Zhang, L. M. Duan, and G. C. Guo, Phys. Rev. Lett. **93**, 240501 (2004).
[20] W. T. Liu, W. Wu, B. Q. Ou, P. X. Chen, C. Z. Li, and J. M. Yuan, Phys. Rev. A **76**, 022308 (2007).
[21] D. F. V. James, P. G. Kwiat, W. J. Munro, and A. G. White, Phys. Rev. A **64**, 052312 (2001).
[22] N. Gisin, G. Ribordy, W. Tittel, and H. Zbinden, Rev. Mod. Phys. **74**, 145 (2002).
[23] C. Kurtsiefer, S. Mayer, P. Zarda, and H. Weinfurter, Phys. Rev. Lett. **85**, 290 (2000).
[24] A. Beveratos *et al.*, Eur. Phys. J. D **18**, 191 (2002).
[25] P. A. Hiskett *et al.*, New J. Phys. **8**, 193 (2006).
[26] H. Rabitz *et al.*, Science **288**, 824 (2000).